

REPORT

CR 86056

CROSS FIELD MAGNETIC MODULATOR

Measurement of Y  
Parameters

Submitted by T. A. O. Gross & Associates

Lincoln, Mass. 01773

in partial fulfillment of

NASA Purchase Order ER-11429

GPO PRICE \$ \_\_\_\_\_

CFSTI PRICE(S) \$ \_\_\_\_\_

SUMMARY

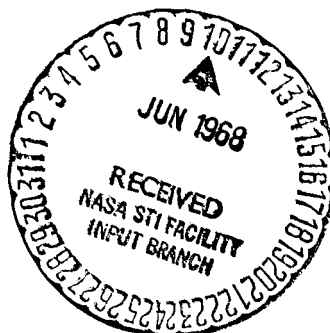
Hard copy (HC) \$3.00

Microfiche (MF) \_\_\_\_\_

ff 653 July 65

The cross field magnetic modulator from a ferrite pot core is a reciprocal device ( $Y_{12}=Y_{21}$ ) when operated with excitation frequency below that of the gyro-magnetic resonance of the ferrite.

No unusual possibilities arising from the device shape anisotropy were noted. However the cross field device appears to offer advantages in both performance and cost over conventional reactors in high-frequency magnetic amplifier and modulator applications.



Submission date:

28 February 1968

4  
N 98-2532  
(ACCESSION NUMBER)  
26152  
(PAGES)  
CV 86152  
(NASA CR OR TMX OR AD NUMBER)  
(THRU)  
(CODE)  
(CATEGORY)

FACILITY FORM 602

## Introduction

In conventional saturable reactors the flux in the magnetic circuit due to the exciting current and that due to the modulating current are in parallel. In order to use conventional reactors in magnetic amplifiers or modulators it is necessary to arrange them in matched pairs.

The cross field reactor places the exciting field perpendicular to the modulating or signal field. The corresponding circuits are uncoupled and the need for balancing with matched pairs is eliminated. Material utilization is doubled and costs of selection are eliminated.

The cross field concept is old. Burgess and Frankfield described the decoupling of a d-c control circuit from an excitation winding by perpendicular fluxes in a U.S. Patent (720,884) filed in 1901. All of the relevant literature on cross field devices known to us appears in the brief list in Appendix A. The lack of interest has been due to difficulty in handling orthogonal fluxes in laminated core materials.

The development of really good ferrites which have low loss without lamination permit efficient cross field devices by virtue of core isotropy. It was this new opportunity which prompted the measurements reported herein.

The principal investigator was Winthrop Gross. Bronislaw Szpakowski consulted on certain aspects of the measurement and applications study. The cross field reactor configuration was conceived by T. A. O. Gross prior to the present program.

## Device Description

The device subjected to the Y parameter measurements reported herein is similar to those illustrated in Fig. 1. The core is an Allen-Bradly C2400D207A modified by enlargement of the center hole to 5/16" ID. This modification is necessary to accommodate the toroidal windings.

The bobbin coil is 244 turns of Ga. 19; the two parallel toroidal windings are 26 turns each of Ga. 21.

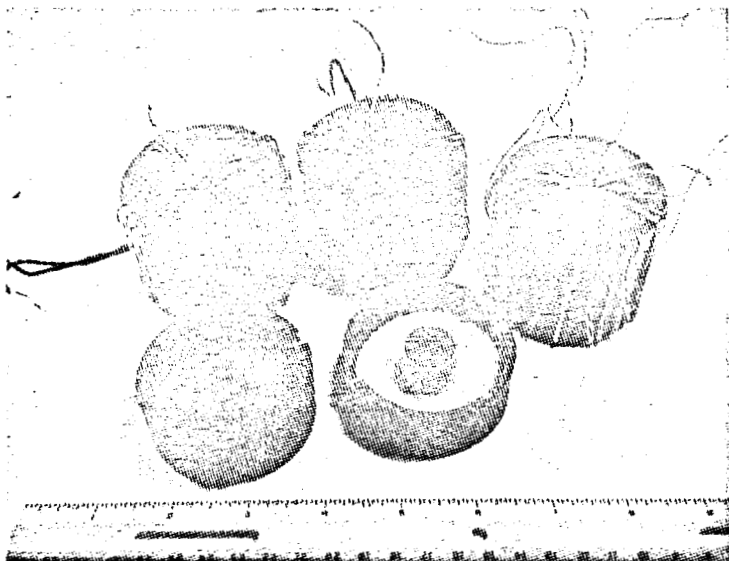


Fig. 1

Cross field reactors.  
Unit on right is similar to device tested for Y parameters.

Bridge measurements on this device are:

Bobbin Winding (Leads B&B)

95 millihenries,  $Q=34$  @ 1 kHz GR Model 650-A  
0.6 ohms d-c " " "  
Z=215 ohms, 87.5 degrees @ 400Hz Acton 310  
Z Angle Meter

Toroidal Winding (Leads T1 to T1 and  
T2 to T2 taken Separately)

25 millihenries,  $Q$  2.4 @ 1 kHz, GR 650-A  
0.31 ohms d-c " " "  
Z=27.3 ohms, 85.9 degrees @ 400 Hz Acton 310A

The above readings are not affected by the short circuiting of the idle windings with the obvious exception of the bifilar toroidal windings. This attests to the excellent isolation afforded by the perpendicular fields.

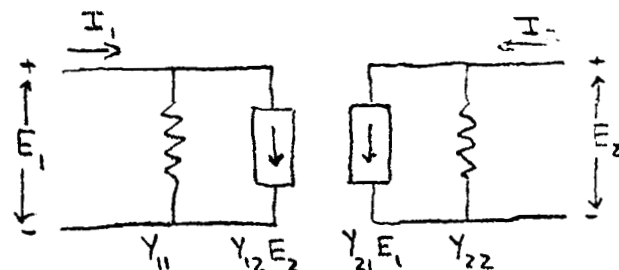
Appendix B contains copies of graphs of device characteristics which were first shown in our July 1967 proposal. They are included here for convenience. Appendix C contains Allen-Bradley technical data on the W-04 ferrite material.

The magnetic path length to flux produced by the bobbin coil ampere-turns is 20.3 cm. Thus the magnetizing force due to bobbin current =  $(244/20.3) I = 12 I$ . The magnetizing force produced by the toroidal windings varies inversely with the radial distance. The magnetic path for the inside of the center hole is 2 cm; for the center post OD it is 4.6 cm. The magnetic path length for outermost diameter is 15.5 cm.

Interpretation of the measurement results is aided by bearing in mind that the center post begins to be saturated (10 amp-turn/cm) with  $I_t = 10 \times 2\text{cm}/26$  Turns or at approximately 800 milliamperes. The entire core is substantially saturated with about 6 amperes in one of the 26 turn toroidal windings. Owing to the dependence of core geometry upon MMF the symbol  $H_t$  has been used on the graphs loosely.  $H_t$  must be calculated by the procedure given above when contemplating MMF caused by the toroidal winding in a particular region of the core.

### Y Parameters

The determination of the Y parameters of a linear device is required to specify completely its circuit characteristics. The defining equations and circuit model for a two port linear device characterized by Y-parameters are shown in Figure 2. The Y parameters of a pot core geometry, cross field reactor were measured in order to fit it into the standard model for the linear two-port. Aside from the formulation of a linear model for the device, the Y-parameters provide a straightforward indication of whether the device is inherently active or passive. The Y-parameters were measured using the simplest methods available in order to reduce the possibility of making a large error while seeking unneeded precision. The four parameters are designated  $Y_{11}$ ,  $Y_{22}$ ,  $Y_{12}$ ,  $Y_{21}$  with  $Y_{11}$  being the admittance of the toroidal winding and  $Y_{22}$  being the admittance of the bobbin winding. Each Y-parameter will be discussed individually as to methods used and results obtained.



$$I_1 = Y_{11} E_1 + Y_{12} E_2$$

$$I_2 = Y_{21} E_1 + Y_{22} E_2$$

Figure 2 - Y-parameter two-port model

### $Y_{11}$ , (Short-circuit input impedance)

In accordance with the convention established above, the toroidal winding is designated the input of the device. The measurement scheme is shown in Fig. 3. An impedance bridge with its internal generator set at 1 kHz was connected one of the toroidal windings. The other toroidal winding was connected to a current source. The bobbin coil was connected to a low impedance power supply. The inductance and Q of the

input were measured at various bias currents, and then converted into the conductance and susceptance of  $Y_{11}$ .  $Y_{11}$  is plotted in Figure 4 for  $I_b=0$  and 1 ampere; values of  $Y_{11}$  for  $0 < I_b < 1$  ampere lie between the curves shown. The admittance increases with toroidal magnetization as would be expected with decreasing permeability of the core. The ratio  $-\text{Im } Y_{11}$  to  $\text{Re } Y_{11}$  is plotted on the same graph. This ratio =  $Q$  which initially increases, peaks and finally falls off for magnetizations  $> 15$  ampere-turns.

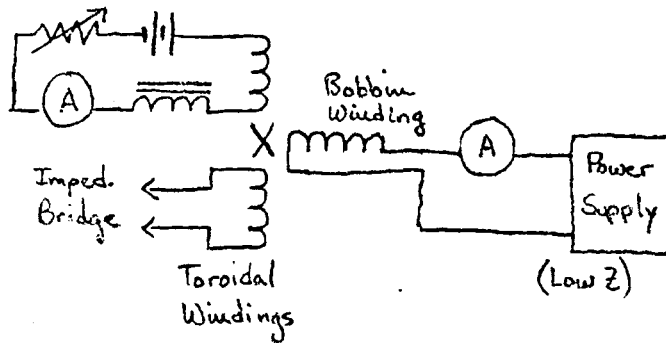


Figure 3- Measurement scheme,  $Y_{11}$  showing connection of bias supplies

An interesting region of graph in Fig. 4 is that for magnetizations between 10 and 20 ampere-turns. Note that the curves for  $I_b=0$  and  $I_b=1$  ampere crossover at 12 ampere-turns for both real and imaginary parts of the admittance. This crossover occurs at about the same magnetization as that for maximum  $Q$ . This is possibly a region which should be more

fully investigated to determine if there is a correlation.

#### $Y_{12}$ (Reverse, short circuit, transadmittance)- Measurement Scheme

The method used is diagrammed in Figure 5. The bobbin winding was driven with a 25 watt amplifier through an isolating resistive pad and a large d-c blocking capacitor. The d-c bias was delivered by a current source.

The current in the toroidal winding was measured with a high-frequency current transformer with a primary admittance of about 20 mhos, thus assuring an effective short circuit. The second toroidal winding was connected as in the measurements of  $Y_{11}$ . The a-c toroidal current was determined at several a-c bobbin voltages and a limit to the infinitesimal input taken.

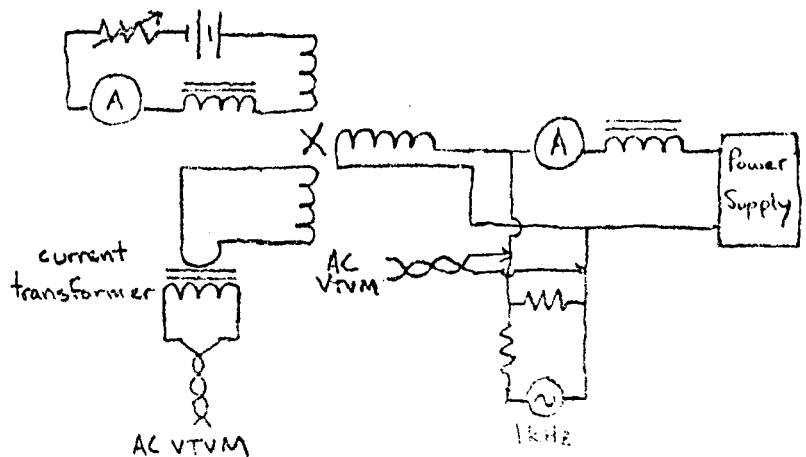
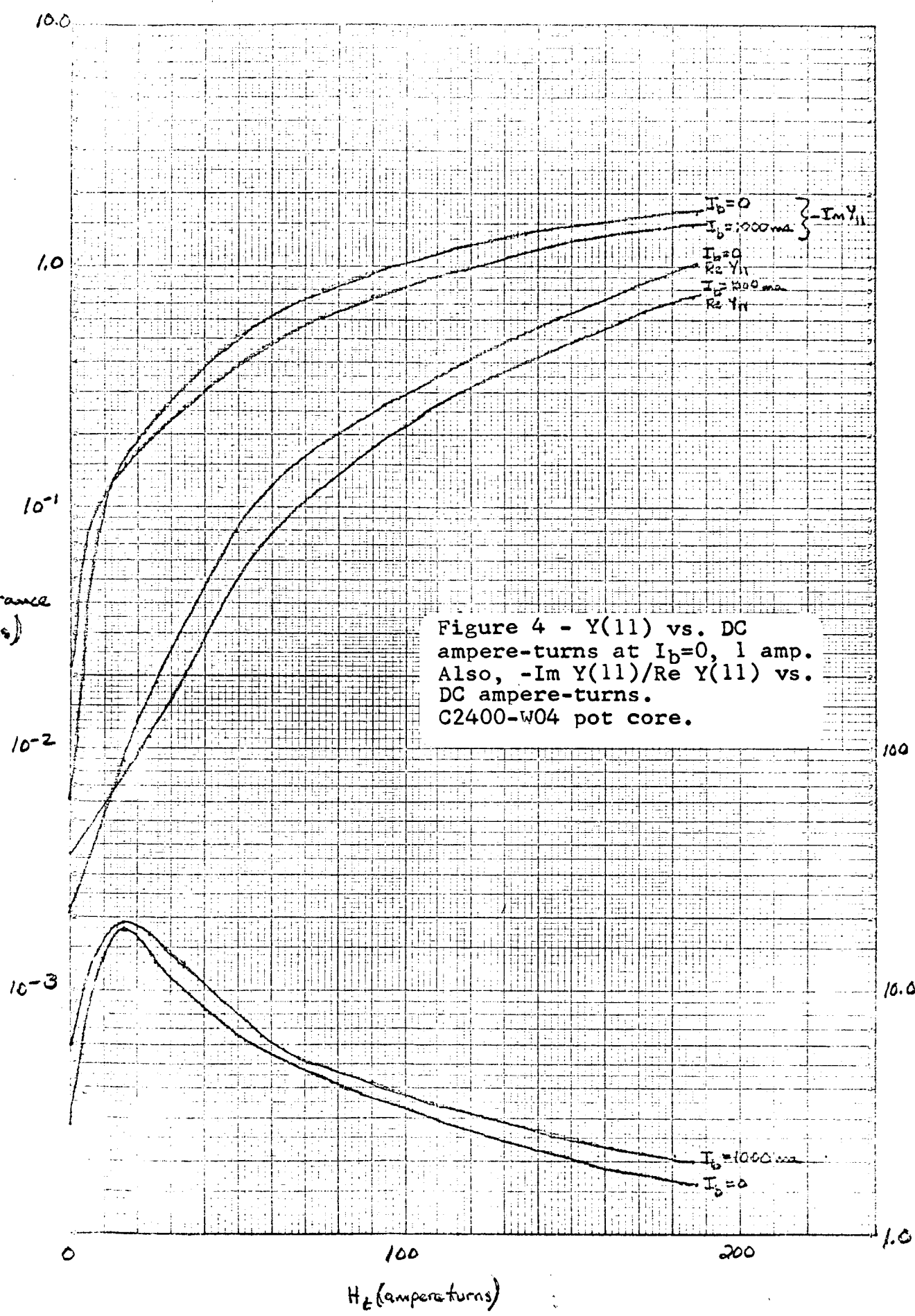


Figure 5- Measurement scheme,  $Y_{12}$

PRINTED IN U.S.A.



$Y_{11}$  Admittance (mhos)



$-\frac{\text{Im } Y_{11}}{\text{Re } Y_{11}}$

These measurements give only the magnitude of the transadmittance; the phase angle was determined with oscilloscope lissajous patterns.

#### $Y_{21}$ (Reverse, short circuit, transadmittance)- Measurement scheme

The measurement scheme for  $Y_{21}$  is similar to that devised for  $Y_{12}$ ; it is diagrammed in Fig 6.

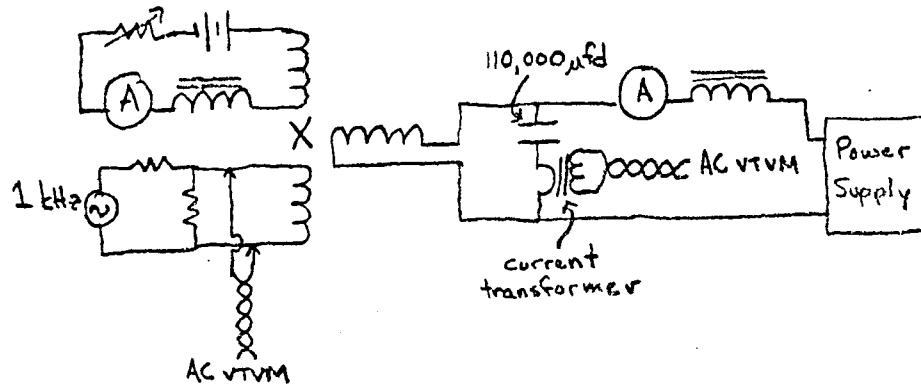


Figure 6 - Measurement scheme,  $Y_{21}$

In this case the toroidal winding is driven and the current transformer is connected across the bobbin.

#### $Y_{12}$ and $Y_{21}$ Results

The magnitude of the transadmittance parameters are displayed in Figures 7 & 8. The phase angles are plotted in Figure 9. The first and most important feature to be noted in these curves is that the magnitudes are substantially identical (within experimental accuracy). Therefore the cross field reactor can be characterized as a reciprocal and as an inherently passive device- at least over the range of bias currents measured. This does not, of course, rule out the possibility of amplification in the standard magnetic amplifier configuration. The behaviour of the transadmittances for very small magnetizations are graphed in Figures 10 & 11 because there were early indications that the transadmittances were not equal in these regions. These indications turned out to be unfounded as shown by the graphs. The most striking feature of these curves is the wide excursion of transadmittance with magnetization, both toroidal and bobbin.

Phase measurements of  $Y_{12}$  and  $Y_{21}$  show considerable discrepancy. This is believed to be due to error in measurement due to distortion. Large input signals were required to produce readable patterns and distortion was observable at these input levels.



$|Y_{12}|$   
Admittance  
(mhos)

1.0

$10^{-1}$

$10^{-2}$

$10^{-3}$

$I_b = 1000$

$I_b = 200$

$I_b = 50$

$I_b = 1000$  ma

$I_b = 200$  ma

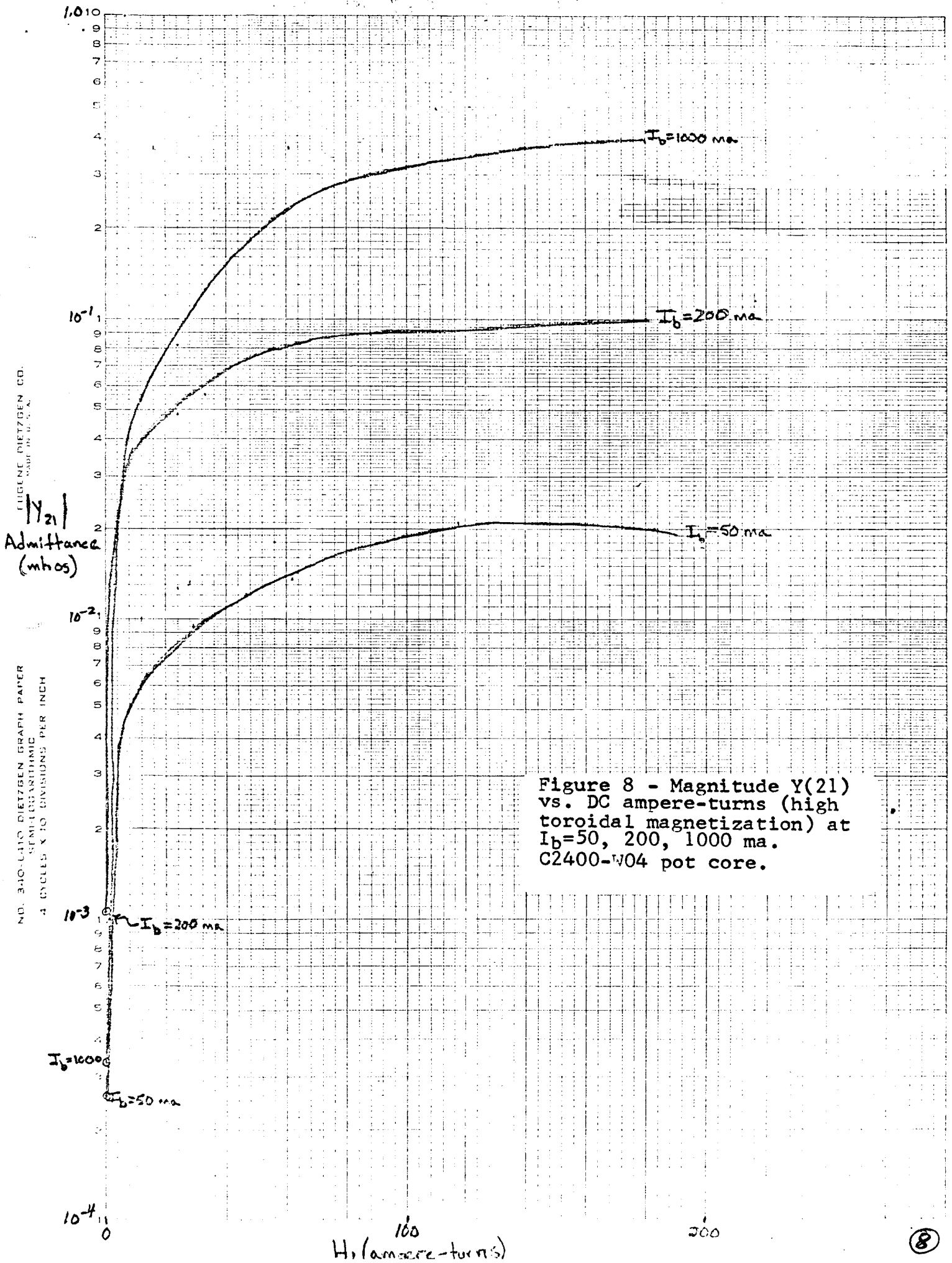
$I_b = 50$  ma

Figure 7 - Magnitude  $|Y_{12}|$  vs. DC ampere-turns (high toroidal magnetization) at  $I_b = 50, 200, 1000$  ma. C2400-W04 pot core.

$H_x$  (ampere-turns)

200





$Y_{12}, Y_{21}$   
Phase  
Shift (degrees)

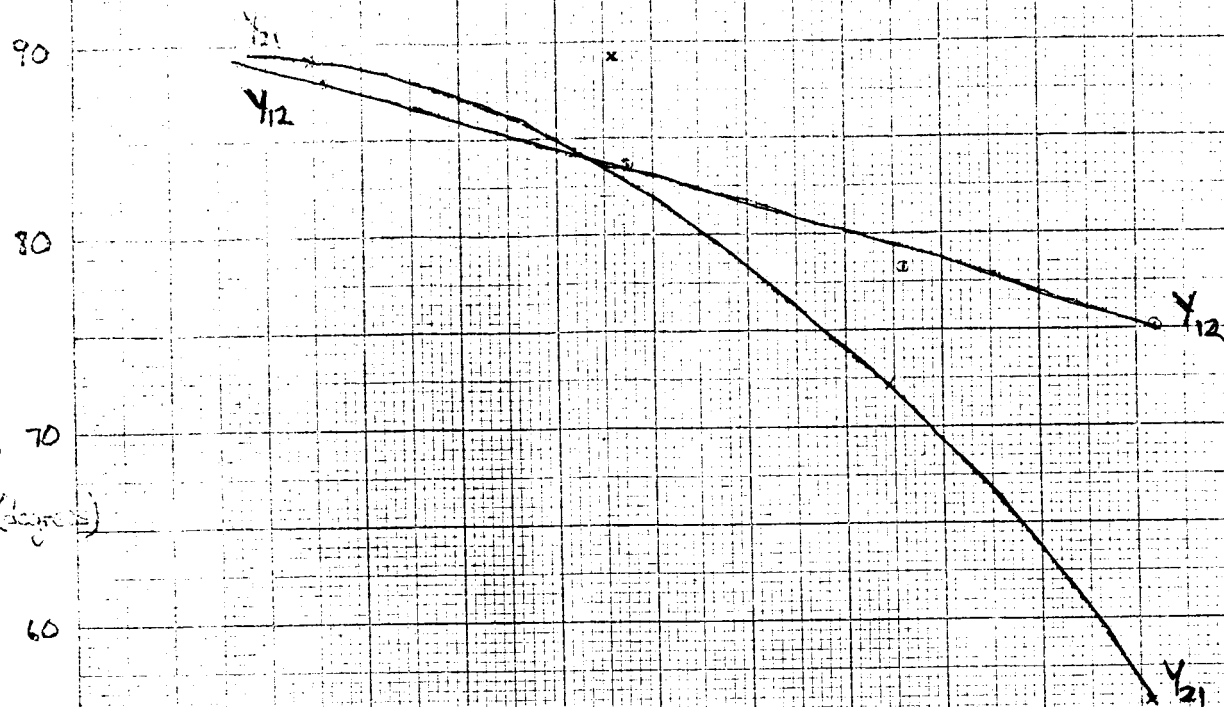


Figure 9 - Phase angle of  $Y(12)$  and  $Y(21)$  vs. DC ampere-turns for  $I_b=200$  ma. C2400-W04 pot core.

10000

1000

100

10

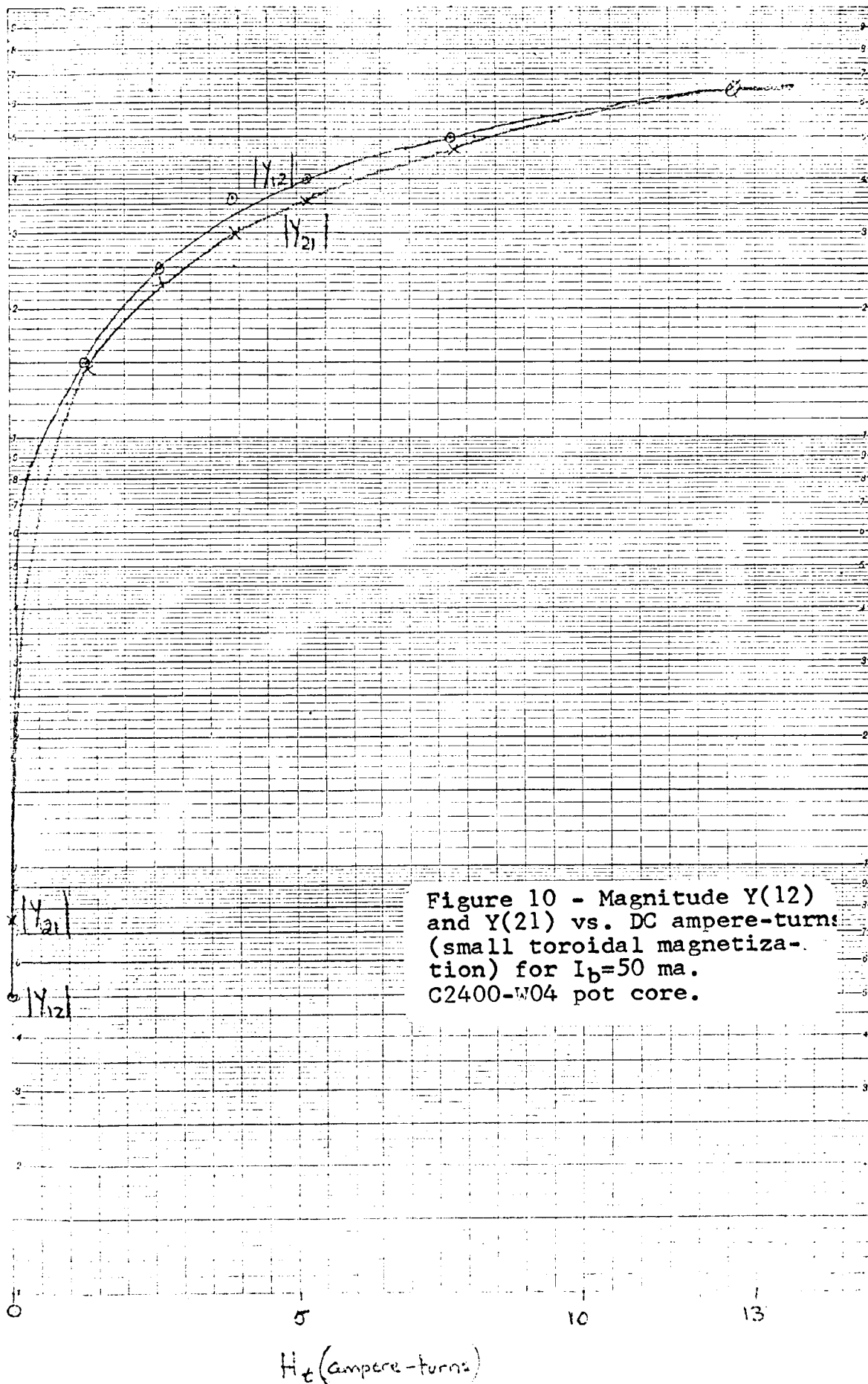
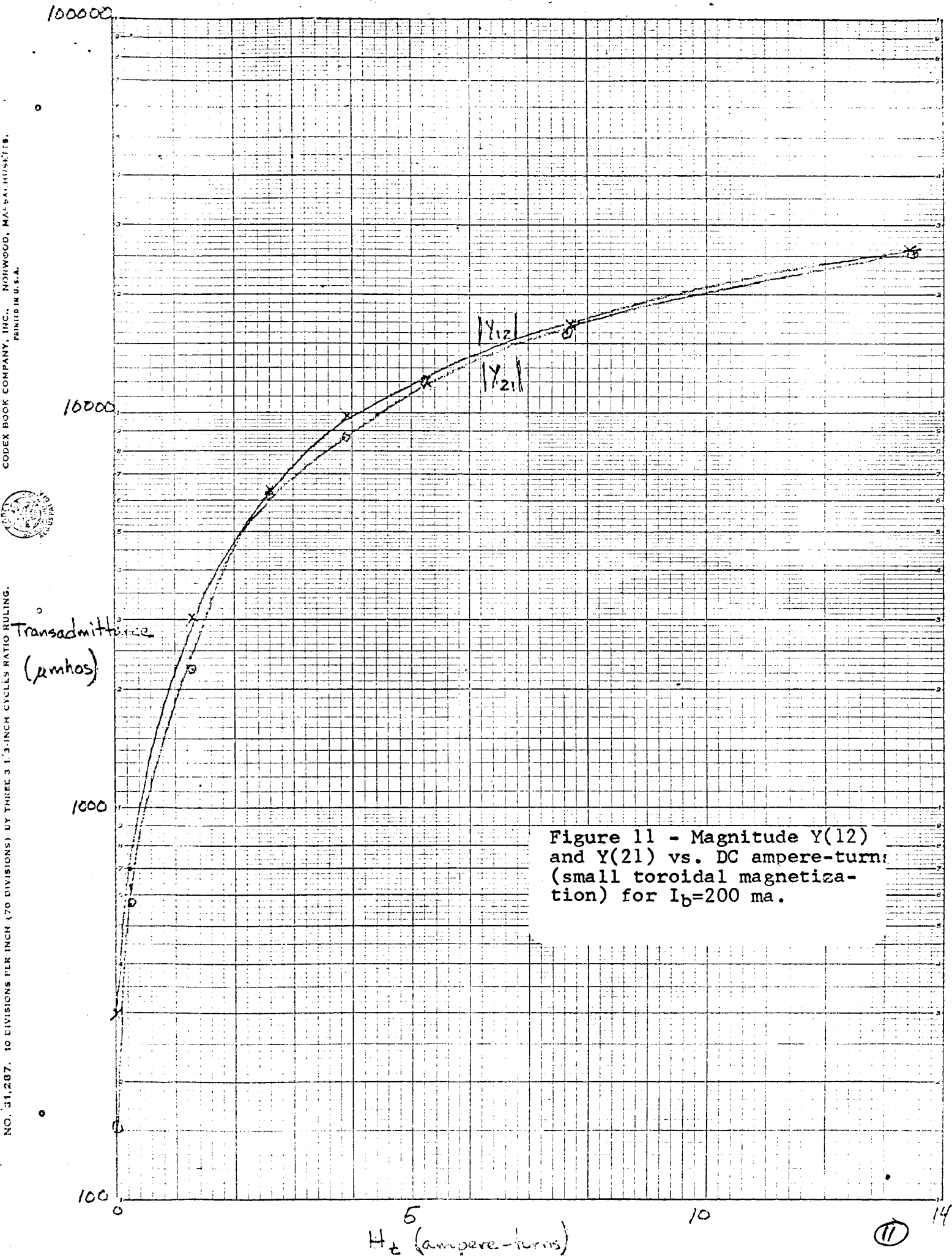
Transadmittance  
( $\mu\text{mhos}$ )

Figure 10 - Magnitude  $Y(12)$  and  $Y(21)$  vs. DC ampere-turns (small toroidal magnetization) for  $I_b = 50$  ma. C2400-W04 pot core.





The phase shift is seen to be in the neighborhood of 90 degrees which is further evidence that the trans-admittance is attributable to modulation of the core permeability rather than to inductive coupling.

$Y_{22}$  (Output, short-circuit, admittance)

The measurement setup is shown in Figure 12. The impedance bridge is connected across the bobbin winding whose d-c bias is supplied from a high-impedance source. The toroidal winding is shorted. The results are plotted in Fig. 13.

The striking feature for these curves is the behaviour of the imaginary parts for different bobbin currents. For little or no bobbin current the susceptance increases with magnetization. This should be expected due to the decreasing permeability of the core. However, for higher bobbin currents the susceptance decreases. A possible explanation is that the ferrite is initially saturated but the toroidal winding unsaturates the core, resulting in reduced susceptance. This effect was not observed for  $Y_{11}$ , perhaps because the magnetization was not as great.

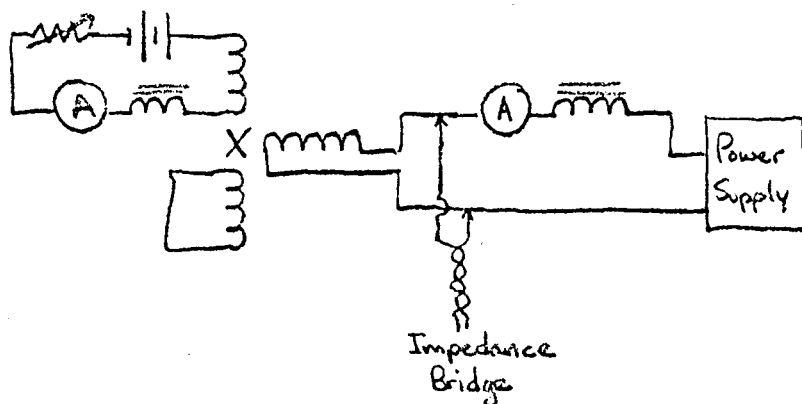


Figure 12- Measurement scheme,  $Y_{22}$

PRINTED IN U.S.A.



10 DIVISIONS PER INCH (120 DIVISIONS) AT 3 1/2 INCH CIRCLES PER INCH

$Y_{22}$   
Admittance  
(mhos)

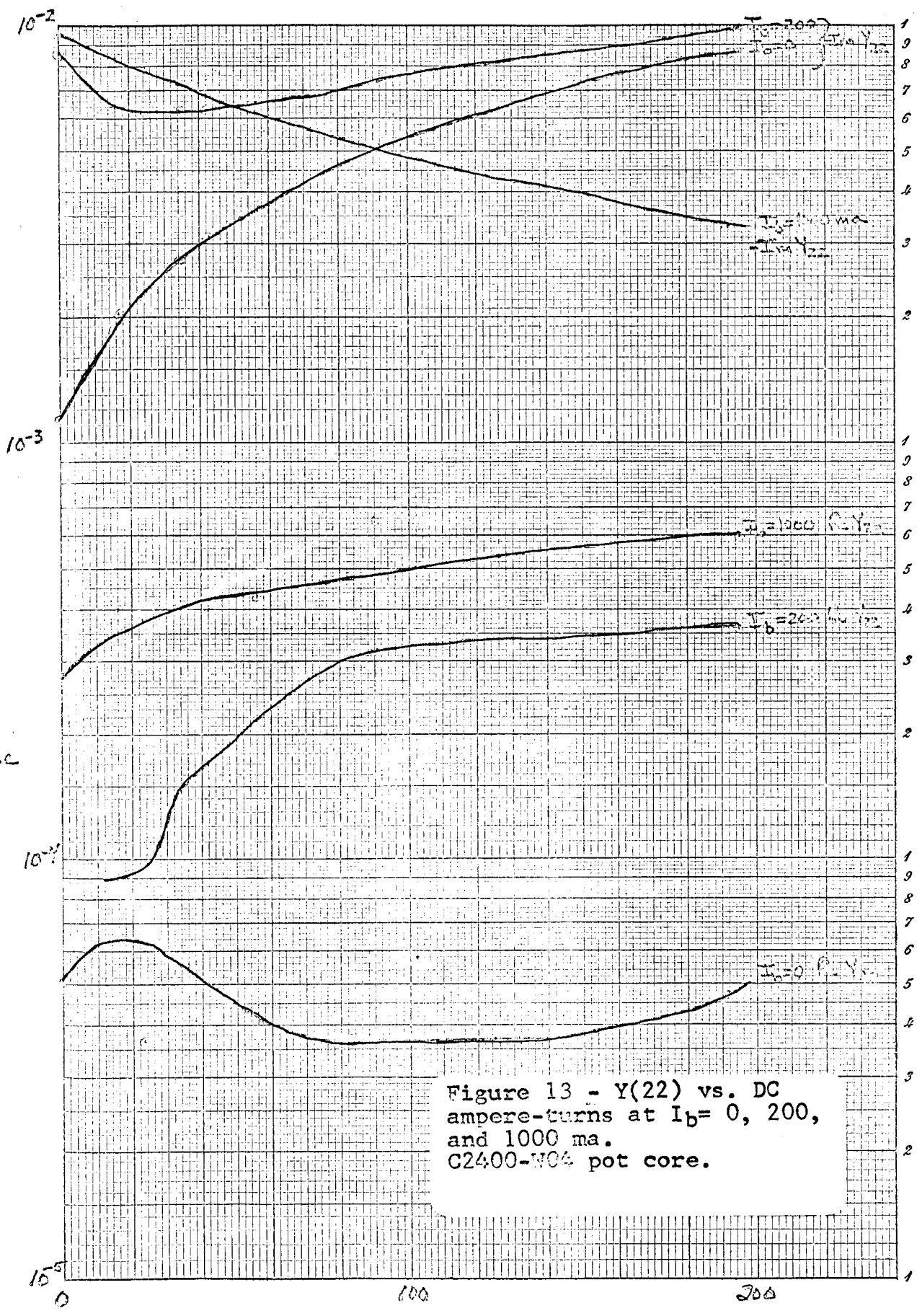


Figure 13 -  $Y(22)$  vs. DC  
ampere-turns at  $I_b = 0, 200,$   
and 1000 ma.  
C2400-W04 pot core.

### Gyromagnetic Resonance

Strong coupling has been observed between the bobbin and toroidal windings when the device is operated near the gyromagnetic resonance frequency. This frequency is proportional to  $H$  and for W-04 materials it extends into the megacycle region with high magnetizations. The minimum frequency for W-04 ferrite appears to be in the order of 100 kHz. Crystalline anisotropy is believed to be the mechanism taking over as  $H$  approaches 0. The Y-parameters were taken at 1 kHz which is well removed from the gyromagnetic resonance frequency. Precautions against hysteresis effects were by de-magnetizing the core with a decaying 60 Hz field following each set of measurements.

Although efforts were made to eliminate effects of gyromagnetic resonance it is quite possible that useful applications could be made with cross-field devices operating in the region. A current tunable band-pass filter is one possibility.

## APPENDIX A

### Bibliography on Cross Field Devices

F. J. Beck and J. M. Kelly, "Magnetization in Perpendicularly Superposed Direct and Alternating Fields," Journal Of Applied Physics, Vol 19, pp. 551-562, June 1948

E. H. Frei, S. Shtrikman, and D. Treves, "A Transducer Using Crossed Magnetic Fields" Bulletin of the Research Council of Israel (Jerusalem, Israel), p. 443, March, 1954, and "A Clip-On Milliamperemeter for D-C Currents", ibid., p. 444

C. F. Burgess and B. Frankenfield, "Regulation of Electric Circuits," U. S. Patent #720,884, Filed June 12, 1901

R. A. Heartz and H. Buelteman, Jr., "The Application of Perpendicularly Superposed Magnetic Fields," AIEE Transactions, Vol. 74, Part I, pp. 655-659, Nov. 1955





T. W. O. GROSS & ASSOCIATES

JUL 29 1967

